International Journal of Electrical and Computer Engineering (IJECE)
Vol. 15, No. 2, April 2025, pp. 1396~1410
ISSN: 2088-8708, DOI: 10.11591/ijece.v15i2.pp1396-1410

Comparison design of dynamic voltage restorers, distribution static compensators and unified power quality conditioner series shunts on voltage sag, and voltage swell

Yulianta Siregar[1], Syahrun Mubarok[1], Nur Nabila Mohamed[2]
[1]Department of Electrical Engineering, Faculty of Engineering, Universitas Sumatera Utara, Medan, Indonesia
[2]School of Electrical Engineering, College of Engineering, University Technology MARA, Shah Alam, Malaysia

Article Info

Article history:

Received Jul 18, 2024
Revised Dec 6, 2024
Accepted Dec 14, 2024

Keywords:

Distribution static compensator
Dynamic voltage restorer
Unified power quality conditioner
Voltage sag
Voltage swell

ABSTRACT

One issue with the power system is electrical power quality, which is brought on by short circuit disruptions and growing nonlinear loads. Power systems frequently have short circuits, resulting in voltage sags that can harm delicate loads. Voltage sage and swell issues can be resolved using unified power quality conditioner series shunts (UPQC-S), distribution static compensators (DSTATCOM), and dynamic voltage restorers (DVR). Custom power devices are very useful in overcoming problems with electrical networks. In this research, due to 3-phase short circuit faults, voltage sag and swell simulations were conducted using a load equal to 70% of the total load and a fault location point of 75% of the feeder length, from the results of research conducted with the case study PT. PLN (Persero) UP3 Sibolga Feeder SB 02 shows that DVR performs better than DSTATCOM and UPQC-S in handling voltage sag and voltage swell due to 3-phase short circuit disturbances. The DVR succeeded in providing the largest voltage sag recovery in phase C, increasing the voltage from 0.2481 pu to 0.9776 pu. The DVR is also effective in overcoming voltage swell on phase A, reducing it from 1.724 pu to 0.9969 pu.

Corresponding Author:

Yulianta Siregar
Department of Electrical Engineering, Faculty of Engineering, Universitas Sumatera Utara
Dr. T. Mansur No. 9, Medan City, North Sumatera Province 20222, Indonesia
Email: julianta_srg@usu.ac.id

1. INTRODUCTION

Nowadays, electricity is a source of energy that people widely use to carry out daily activities. High electricity demand must also be balanced with the availability of electricity for consumers through a reliable and high-quality electricity distribution system [1]–[3]. The distribution system is a part of the electrical system that distributes electric power from the substation to consumers. Even though power quality is an important aspect to pay attention to when considering the many problems in the electric power system.

Power quality and voltage stability are the primary issues with electric power systems. Power quality is a critical component of power distribution systems due to the extensive use of power electronics. The growing use of non-linear electronic loads is the primary cause of power quality issues. Issues with the electric power system's power quality include voltage sag, voltage swell, interruptions, current harmonics, and voltage harmonics [4]–[6]. Power quality issues like voltage sag and swell frequently arise when disturbances occur in distribution networks. An electrical system phenomenon known as voltage sag occurs when the root-mean-square (RMS) value drops from 10% to 90% of the normal voltage briefly, ranging from 0.5 cycles to 1 minute. This is known as a voltage swell when the RMS voltage rises from 110% to 180%

throughout 0.5 cycles to 1 minute. A short circuit in the electric power system or starting motor is one of the reasons for voltage sag, whereas significant load variations result in voltage swell [7]–[9].

With advances in power electronics and control applications. Considering that the phenomenon of voltage sag and voltage swell is a disturbance that can cause damage to electrical equipment and affect the overall performance of electrical power quality, a sensitive load protection device is needed to improve power quality. A special power device is installed on the distribution channel to maintain the stability of electrical power when there is a disturbance to the source or load. Numerous power device types, including distribution static compensators (DSTATCOM), static var compensator (SVC), dynamic voltage restorer (DVR), and unified power quality conditioner (UPQC), are specially designed to improve power quality [10]. In order to address the issues of voltage sag and swell, this study compares the most efficient special power devices in a 20 kV distribution system. These devices include the DVR, DSTATCOM, and unified power quality conditioner (UPQC) [11]–[13].

Previous research regarding the comparing DVR, UPQC, and DSTATCOM to reduce voltage sag in distribution systems [14]. It discusses problems and errors due to voltage sags in distribution systems using the DSTATCOM, DVR, and UPQC installation methods as devices proven to maintain power quality in the system. Then previous research on load voltage control employed a comparison between DVR and DSTATCOM [15]. The research analyzes the comparison of DVR and DSTATCOM to address power quality and suitability for distribution systems. It is necessary to record the direct-current (DC) storage device rating on the DVR and DSTATCOM correctly for more accurate analysis results and better power quality. Then, further previous research was conducted regarding voltage sags caused by 1-phase, phase-to-phase, and 3-phase short circuits and the impact of installing a DVR. Based on the research results, the biggest disturbance occurs when there is a 3-phase short circuit with a load condition of 70% and when the fault location is 75% at PT. PLN (Persero) UP3 Sibolga Feeder SB 02. Then, previous research about DVR and DSTATCOM were compared and simulated to mitigate voltage sag at distribution [16]. The research discusses the problem of voltage sag interference and provides a comparative analysis of mitigation devices, namely DVR and DSTATCOM, in overcoming voltage sag. The device has been proven to reduce interference problems due to voltage sag. Furthermore, previous research discussed particle swarm optimization and artificial neural networks for voltage sag mitigation in DVR quality improvement analysis [17]. It discusses a case study at PT. PLN (Persero) UP3 Sibolga Feeder SB 02. The research developed a control system for DVR, namely proportional integral-particle swarm optimization (PI-PSO) and artificial neural network (ANN), which recovered disturbances caused by voltage sags that occurred from 0.3 pm to 0.9 pm.

In this research, a simulation and analysis were carried out to compare performance installations with the unified power quality conditioner-series shunt (UPQC-S), DSTATCOM, and DVR techniques. These techniques address voltage sag and swell issues brought on by three-phase short circuit faults. The voltage sag and swell simulations are computed using fault locations at 75% of the line length and short circuit disturbances at 70% of the total load. MATLAB-Simulink software was utilized to conduct the simulation at PT. PLN (Persero) UP3 Sibolga Feeder SB 02, situated in the Sibolga main substation.

2. RESEARCH METHOD

This research was conducted on the 20 kV distribution network at the SB 02 Sibolga main substation feeder at PLN (Persero) UP3 Sibolga, North Sumatra Province, Indonesia. Then, the variables observed in this research are the voltage magnitude and waveform before installing the DVR [18]–[20], DSTATCOM [21]–[23], and UPQC-S [24]–[26] and after installing the DVR, DSTATCOM, and UPQC-S. The above variables are observed and compared for the reliability of each device against voltage sags and voltage swells due to 3-phase short circuits.

The first stage in model design is modeling the electricity distribution system to see voltage sags when a disturbance occurs. The modeled distribution system is carried out on the 20 kV SB 02 Feeder network connected to the Sibolga main substation. Distribution system parameters on the SB 02 Feeder can be seen in Table 1. After determining the simulation parameter values, a test model is formed, which is tested using MATLAB–Simulink software. The distribution system model is shown in Figure 1.

The next stage is to incorporate DVR into the simulation after the electric power distribution system has been modeled. Table 2 lists the settings used by the DVR. Modeling the DVR comes next, following the design of the DVR parameters. To determine the impact of inserting a DVR in series between the source and the load and causing a 3-phase short circuit, modeling was done using MATLAB-Simulink. Figure 2 displays the circuit model for the DVR installation. Meanwhile, Figure 3 shows a representation of the DVR circuit.

Table 1. Before and after adjustment, the load voltage in PU and THD for every phase

Component	Parameter
Grid voltage	150 kV
Power transformer	150 kV/20 kV, 60 MVA
Transmission length	33.12 kms

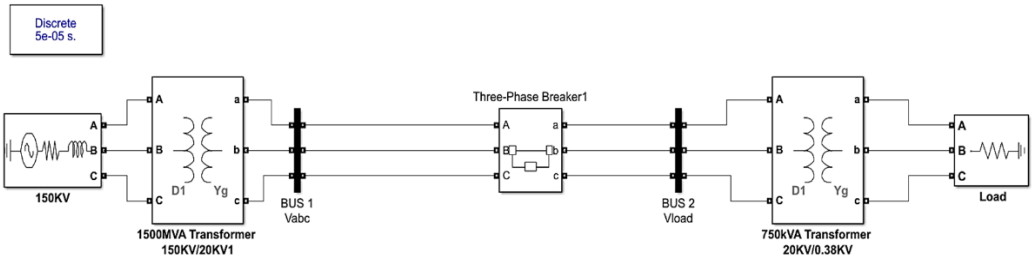

Figure 1. The electric power distribution system model in initial condition

Table 2. Parameters of a DVR

Parameter	Value
Injection transformer	70 kVA, 0.40/20 kV
Resistance	1 Ω
Inductance filter	5 µH
Capacitance filter	10 µF
DC source	2 × 1800 V

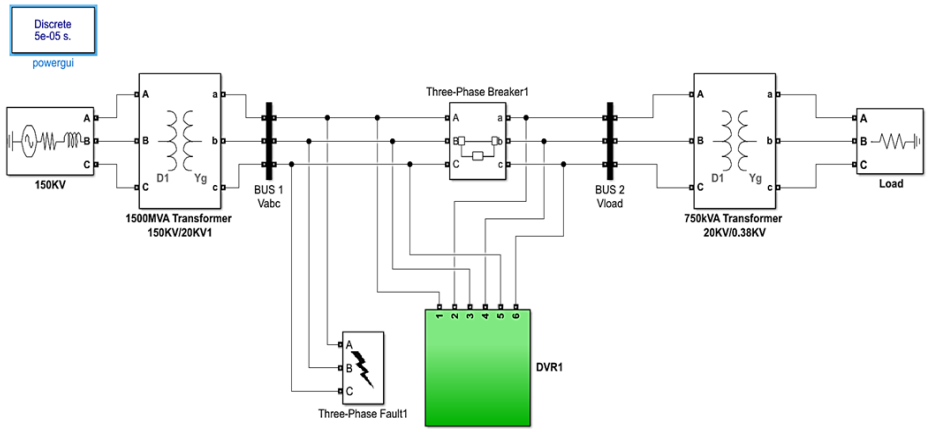

Figure 2. Circuit model after installing the DVR

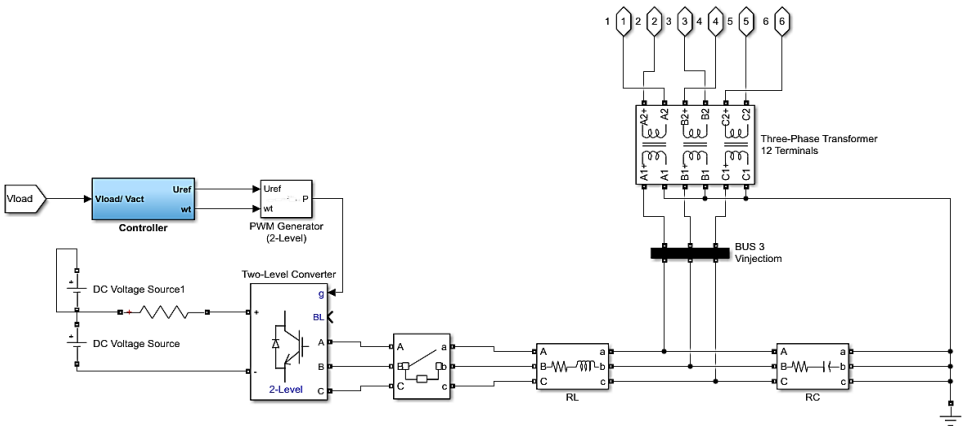

Figure 3. DVR circuit

Table 3 lists the parameters the DSTATCOM utilized. Modeling the DSTATCOM comes next, following the design of the DSTATCOM parameters. To observe the impact of DSTATCOM installation caused by a three-phase short circuit and a shunt installed between the source and the load, modeling was done using MATLAB-Simulink. Figure 4 displays the circuit model for the DVR installation. In the meantime, Figure 5 displays the modeled distribution static compensator circuit.

After modeling the electric power distribution system, the next step is to add the UPQC configuration to the system model. The UPQC-S parameters used are in Table 4. After the UPQC-S parameters are designed, the next step is to model the UPQC-S. Modeling was carried out using MATLAB-Simulink to see the effect of installing UPQC-S due to a 3-phase short circuit and series and shunt installation between source and load. The UPQC-S installation circuit model is shown in Figure 6.

Table 3. Distribution static compensator parameters

Parameter	Value
DC source	$2 \times 1800\ V$
Inductance filter	5 µH
Capacitance filter	10 µF
Injection transformer	70 kVA, 0.40/20 kV

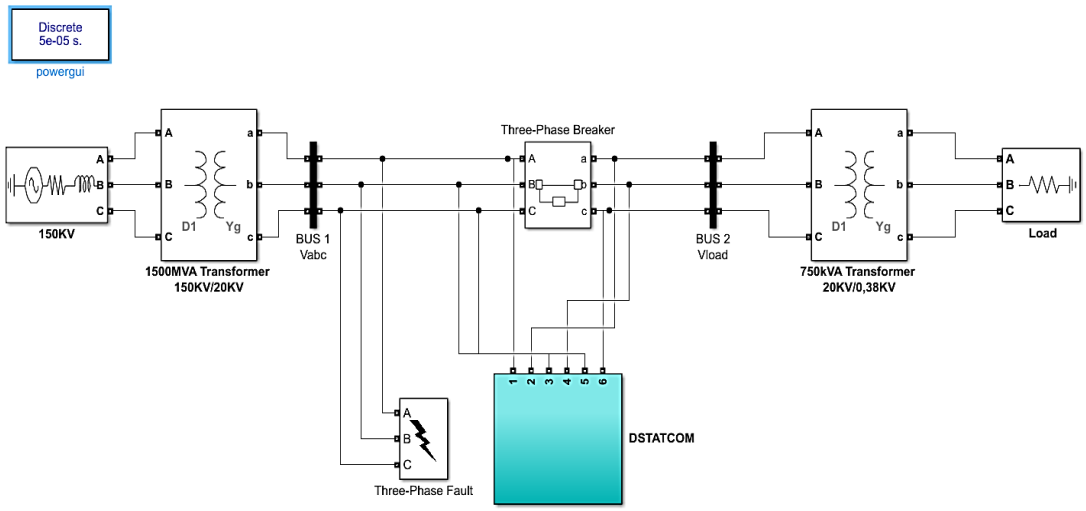

Figure 4. Circuit model after installing the distribution static compensator

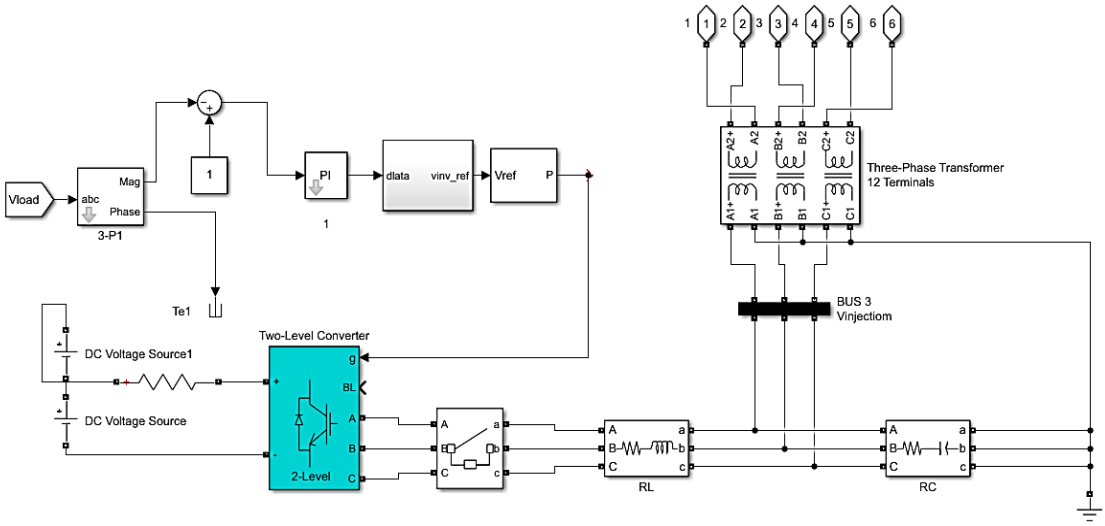

Figure 5. Distribution static compensator circuit

Table 4. Parameters of UPQC-S

Component	Parameter	Value
DC link	Reference voltage	700 V
APF shunt	Coupling inductor	10 μF
	Ripple filter	$R = 10\Omega$
		$C = 10\mu F$
APF series	Ripple filter	$R = 1\ \Omega/\text{phase}$
	Injection transformer	30 kVA, $0.38/20$ kV/phase

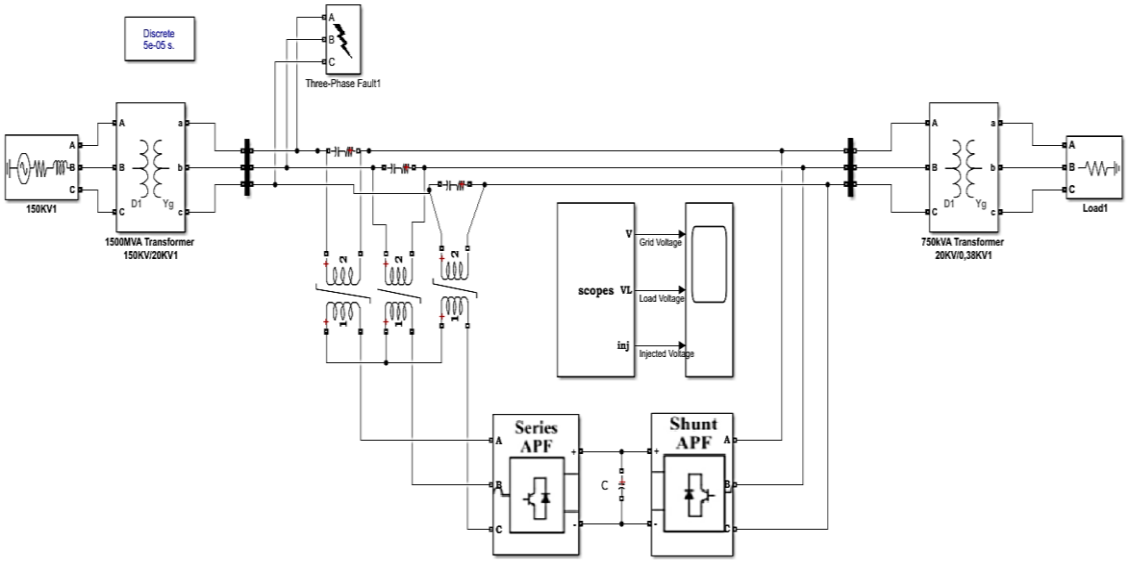

Figure 6. Circuit model after installation of UPQC-S

3. RESULTS AND DISCUSSION

3.1. Calculation of the impedance of the Sibolga substation

Before carrying out a voltage recovery simulation on the system, it is necessary to calculate the impedance to design the distribution system model that will be used and determine the magnitude of the fault current and the location of the fault. The impedance calculations carried out are source impedance, transformer reactance, feeder impedance, and network equivalent impedance. Source impedance calculations were carried out using short circuit data on the primary bus side of the 150 kV Sibolga substation, namely 150 MVA.

3.1.1. Calculation of source impedance

The source impedance is from the peak load current flowing from the power centers to the substation. Finding the short circuit current on the 150 kV secondary side with the source impedance value used is the 150 kV secondary side source impedance value. The source impedance is calculated using short circuit data on the 150 kV primary side bus of the Sibolga substation, which is 150 MVA.

$$X_s = \frac{(\text{kV})^2}{\text{MVA}} \tag{1}$$
$$X_s = \frac{(150)^2}{500}$$
$$X_s = 45\ \text{Ohm}$$

Equation (2) to calculate the source impedance on the 20 kV secondary side.

$$X_{s(20\ \text{kV side})} = \frac{\text{kV(secondary side of the transformer)}^2}{\text{kV(primary side of the transformer)}} \times X_{s(150\ \text{kV side})} \tag{2}$$
$$X_{s(20\ \text{kV side})} = \frac{(20)^2}{(150)} \times 45$$
$$X_{s(20\ \text{kV side})} = 0.8\ \text{Ohm}$$

3.1.2. Calculation of transformer reactance

Source impedance calculations were carried out using short circuit data on the primary bus side of the 150 kV Sibolga.

$$X_{t(\text{at } 100\%)} = \frac{\text{kV(secondary side of the transformer)}^2}{\text{MVA transformer}} \quad (3)$$

$$X_{t(\text{at } 100\%)} = \frac{(20)^2}{60}$$

$$X_{t(\text{at } 100\%)} = 6.6 \text{ Ohm}$$

Positive and negative sequence transformer reactance values.

$$X_{t1} = X_{t2}$$
$$X_t = \% \text{ as known} \times X_t(100\%)$$
$$X_{t1} = 12.78 \times 6.66$$
$$X_{t1} = 0.842 \text{ Ohm}$$

Zero sequence transformer reactance value.

$$X_{t0} = 10 \times X_{t1}$$
$$X_{t0} = 10 \times 0.842$$
$$X_{t0} = 8.42 \text{ Ohm}$$

3.1.3. Calculation of feeder impedance

The feeder impedance is calculated according to the length of the distribution line which consists of positive sequence impedance, negative sequence impedance and zero sequence impedance. The impedance value is calculated using (4) and (5).

$$Z = R + jX\ \Omega/\text{km} \quad (4)$$

$$Z_n = n \times L \times Z/\text{km} \quad (5)$$

The fault location simulation was performed at 75% of the feeder length. The calculation of positive sequence impedance, negative sequence impedance, zero sequence impedance, and feeder length is as follows,

$$\text{Positive sequence impedance, negative sequence impedance} = (0.00 + j0.84)\ \Omega/\text{km}$$
$$\text{Zero sequence impedance} = (120.00 + j8.42)\ \Omega/\text{km}$$
$$\text{Feeder length} = 33.12 \text{ km}$$
$$Z_{n\,(+,-)} = 0.75 \times 33.12 \text{ km} \times (0.00 + j0.84)\Omega/\text{km} = (24.84 + j20.86)\ \Omega$$
$$Z_{n\,(0)} = 0.75 \times 33.12 \text{ km} \times (120 + j0.84)\ \Omega/\text{km} = (2980.1 + j209.15)\ \Omega$$

Thus, Table 5 shows the feeder impedance value for fault locations 75% away.

Table 5. Feeder impedance for fault locations with a distance of 75%

Feeder impedance	Impedance value
Positive and negative sequences	(24.84 + j20.86) Ω
Sequence zero	(2980.1 + j209.15) Ω

3.1.4. Calculation of network equivalent impedance

Equation (6) can be used to calculate network equivalent impedance. Then, $Z_{1\,eki}$ and $Z_{2\,eki}$ can be directly calculated according to the fault location point by adding $Z_s + Z_T + Z_L$.

$$\begin{aligned} Z_{1\,\text{eki}} = Z_{2\,\text{eki}} &= Z_s + Z_T + Z_{1\,\text{feeder}} \\ &= j0.8 + j0.842 + Z_{1\,\text{feeder}} \\ &= j1.642 + Z_{1\,\text{feeder}} \end{aligned} \quad (6)$$

So, the equivalent network impedance value at the location of the 75% fault point is as.

$$Z_{1\,eki} = Z_{2\,eki} = j1.642 + Z_{1\,feeder} = j1.642 + (24.84 + j20.86)\Omega$$
$$= (24.84 + j22.5)\ \Omega$$

Then, the Z_{0eki} calculation is carried out based on the neutral grounding system on the substation side.

Grounding resistance 20 kV is 40 Ω. The Z_0 calculation requires the value of Z_1 of the grounded transformer, neutral resistance R_N, and Z_0 of the feeder. Then, use (7) and (8) to find the value of $Z_0 2$. Meanwhile, Table 6 shows the calculations' conclusions, namely the network's equivalent impedance for the fault location at a distance of 75%.

$$Z_{0\,feeder} = \%length \times Z_0\ total \quad (7)$$

$$Z_{0\,eki} = Z_{t0} + 3R_N + Z_{0\,feeder}$$
$$= j8.42 + (3 \times 40) + Z_{0\,feeder}$$
$$Z_{0\,eki} = j8.42 + 120 + (2980.1 + j209.15)\Omega$$
$$Z_{0\,eki} = (3107.72 + j217.57)\ \Omega \quad (8)$$

Table 6. Network equivalent impedance for fault locations with a distance of 75%

Network equivalent impedance	Impedance value
$Z_{1\,eki} + Z_{2\,eki}$	(24.84 + j22.5) Ω
$Z_{0\,eki}$	(3107.72 + j217.57) Ω

3.2. Calculation of 3-phase short circuit faults

A three-phase fault is a condition where (a) all three phases of the system experience a short circuit with each other, or (b) all three phases of the system are grounded. Generally, this is a balanced condition, and it only needs to know the positive sequence network to analyze the interference. After calculating the impedance at the Sibolga substation, the next step is to calculate the 3-phase short circuit fault current for the 75% fault point based on (9).

$$I = \frac{V}{(Z_{1\,eki})} \quad (9)$$
$$I = \frac{\frac{20000}{\sqrt{3}}}{24.84 + j22.5}$$
$$I = \frac{11547}{33.51 < -42.17}$$
$$I = 344.58 < -42.17\ A$$

3.3. Calculation of voltage sag, and voltage swell

Voltage sag calculations are needed to compare the results of the calculations and the simulations carried out. This calculation is done on a 3-phase short circuit fault for the 75% fault location point. If I_f 3Φ is obtained at the 75% disturbance point, it is $344.58 \times \sqrt{3}$.

$$Z = R + jX = (24.84 + j22.5)\ \Omega$$

So, the voltage sag and voltage swell calculation at the 75% fault point is:

$$V = \sqrt{((75\% \times 24.84)^2 + (75\% \times 22.5)^2} \times 344.58 \times \sqrt{3}$$
$$= 15002\ Volt$$

From the results of the voltage sag calculation for a 3-phase short circuit fault with a fault location point of 75%, the voltage sag obtained is 15,002 Volts.

3.4. Simulation results of voltage sag

The simulation occurs when the three-phase short circuit is based on a load of 70% and the fault location point is 75%. The load percentage results when the load is 70% is 636.65 kVA, and the voltage sag when the fault location is 75% is 15,002 Volts. The voltage sag simulation results consist of several simulations, such as system simulations when a voltage sag occurs after installing DVR, DSTATCOM, and UPQC-S.

3.4.1. Calculation of source impedance

The simulation was conducted for a 3-phase short circuit fault with a load of 70% and a fault location point of 75%. The simulation results are shown in Figure 7. Then, the magnitude of the voltage values of phases A, B, and C that are experiencing interference can be determined using the FFT tools in Simulink MATLAB, as shown in Figures 7. The fundamental voltage of Phase A decreased to 0.3018 pu for a duration of 0.03 to 0.07 seconds. This is caused by voltage sag. Meanwhile, the fundamental voltage of Phase B decreased to 0.2647 pu for a time duration of 0.03 seconds to 0.07 seconds. Then, the fundamental voltage of Phase C decreased to 0.2481 pu for a time duration of 0.03 to 0.07 seconds.

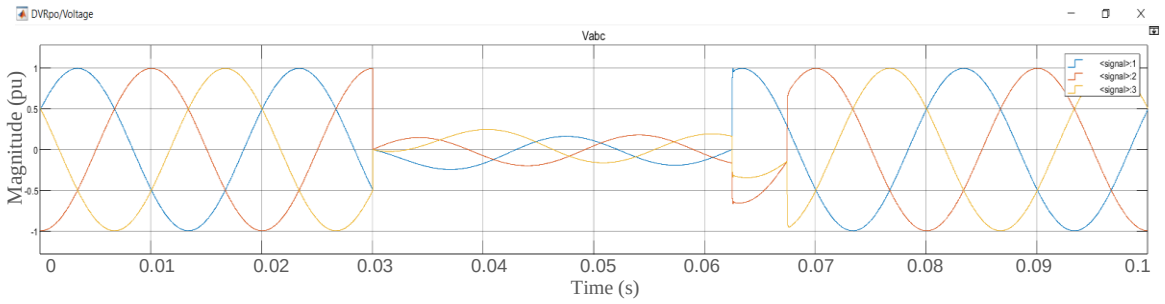

Figure 7. Voltage sag due to 3 phase short circuit

3.4.2. After DVR installation at voltage sag

Simulations were carried out for a 3-phase short circuit fault with a load of 70% and a fault location point of 75% after installing a DVR as a lost voltage restorer. The simulation results are shown in Figure 8. In Figure 8, the voltage value for phases A, B, and C has been restored using a DVR and can be determined using the FFT tools in Simulink MATLAB. The fundamental voltage of phase A after installing the DVR increases to 0.9679 pu. The fundamental voltage of phase B after installing the DVR increases to 0.966 pu. Furthermore, the fundamental voltage of phase C after installing the DVR increases to 0.9776 pu.

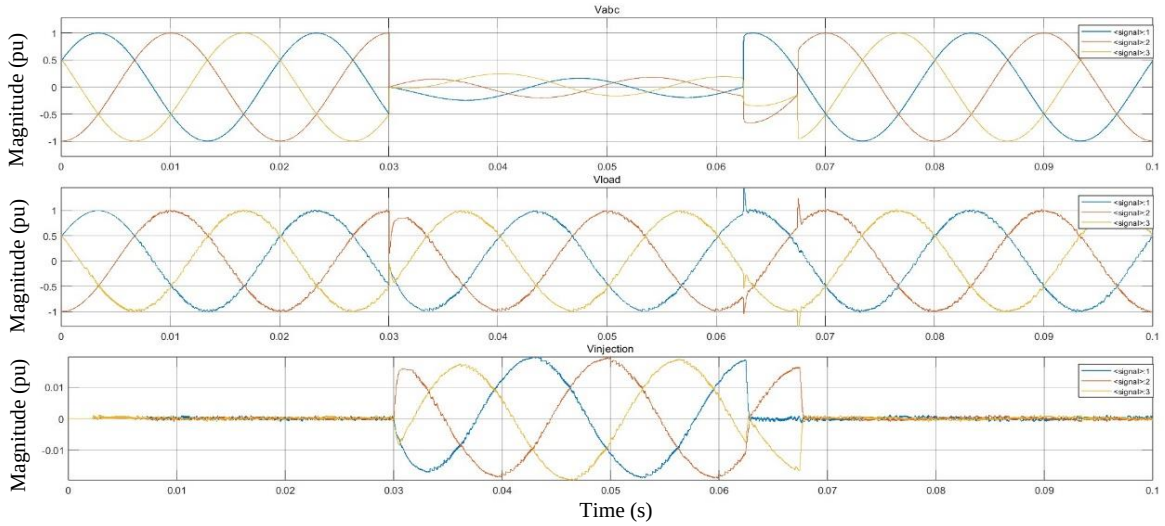

Figure 8. Voltage sag simulation results with DVR

3.4.3. After installation of DSTATCOM at voltage sag

Simulations were carried out for a 3-phase short circuit fault with a load of 70% and a fault location point of 75% after installing DSTATCOM as a lost voltage restorer. The simulation results are shown in Figure 9. Figure 9 shows that the voltage values for phases A, B, and C recovered using DSTATCOM can be determined using the FFT tools in Simulink MATLAB. The fundamental voltage of phase A after DSTATCOM installation increased to 0.7369 pu. Then, the fundamental voltage of phase B after DSTATCOM installation

increased to 0.7235 pu. Furthermore, the fundamental voltage of phase C after DSTATCOM installation increased to 0.7167 pu.

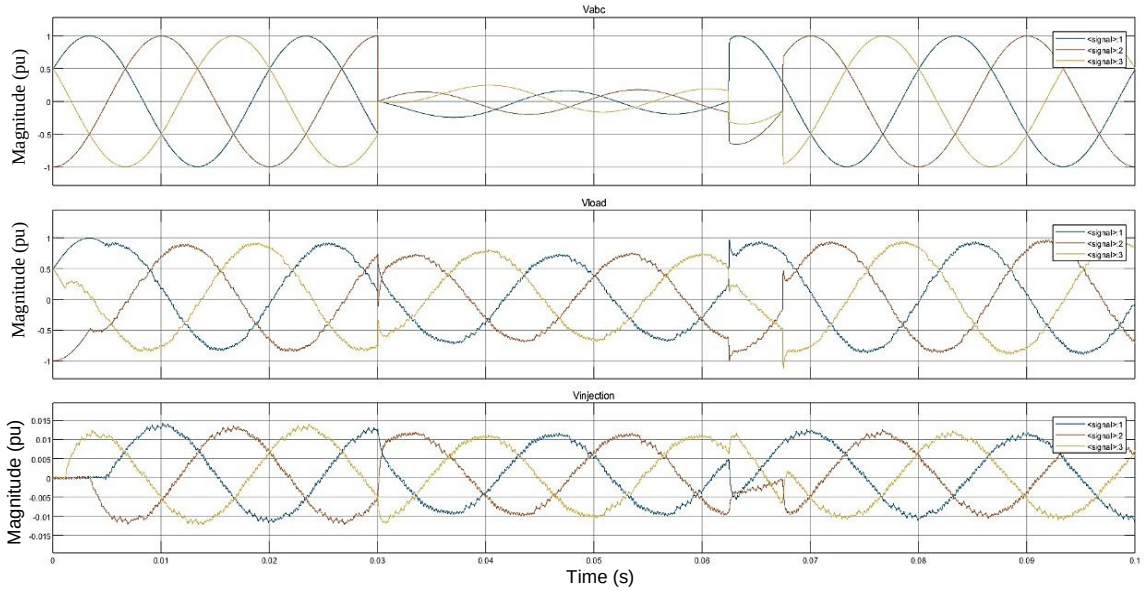

Figure 9. Voltage sag simulation results with DSTATCOM

3.4.4. After installation of UPQC-S at voltage sag

Simulations were carried out for a 3-phase short circuit fault with a load of 70% and a fault location point of 75% after installing UPQC-S as a lost voltage restorer. The simulation results are shown in Figure 10. The voltage values for phases A, B, and C recovered using UPQC-S can be determined using the FFT tools in Simulink MATLAB. The fundamental voltage of Phase A is 318.9 V for a duration of 0.03 to 0.07 seconds, so the fundamental voltage of Phase A is 0.8392 pu (reference voltage 380 Volts). Then, the fundamental voltage of Phase B is 307 V (0.8392 pu) for a time duration of 0.03 to 0.07 seconds. Further, the fundamental voltage of Phase C is 318.8 V (0.8389 pu) for a duration of 0.03 to 0.07 seconds.

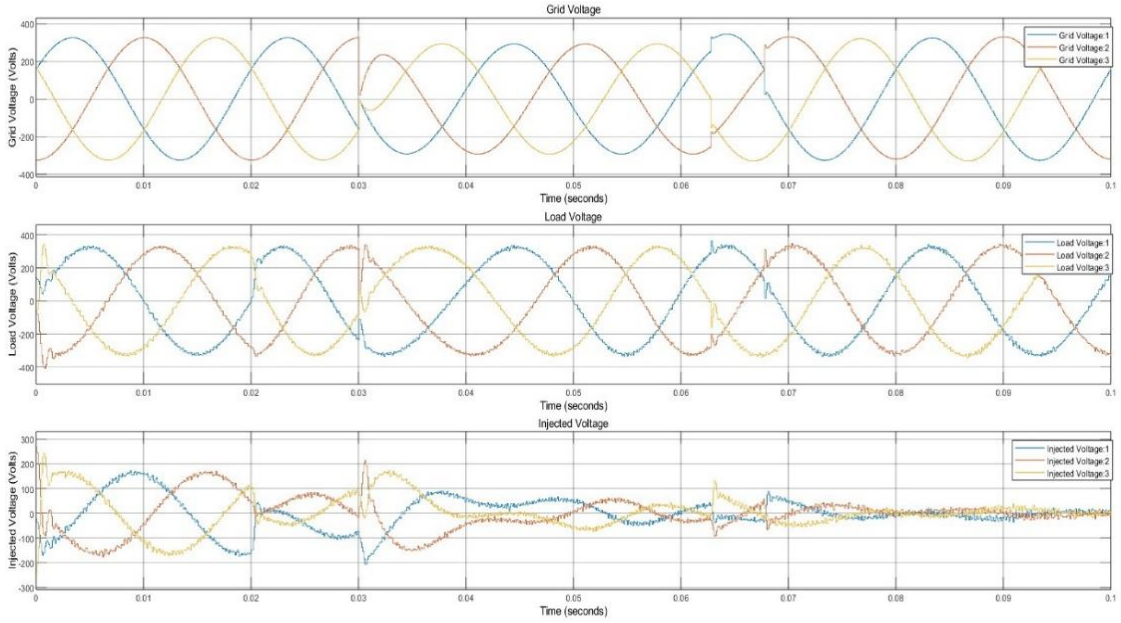

Figure 10. Voltage sag simulation results with UPQC-S

3.5. Simulation results of voltage swell

The simulation occurs when the three-phase short circuit is based on a load of 70% and the fault location point is 75%. The load percentage results when the load is 70% is 636.65 kVA, and the voltage sag when the fault location is 75% is 15,002 Volts. The voltage swell simulation results consist of several simulations, such as system simulations when a voltage swell occurs after installing DVR, DSTATCOM, and UPQC-S.

3.5.1. System simulation results when a voltage swell occurs

The simulation was conducted for a 3-phase short circuit fault with a load of 70% and a fault location point of 75%, as shown in Figure 11. The voltage values of phases A, B, and C that experience voltage swell can be determined using the FFT tools in Simulink MATLAB, as shown in Figures 11. The fundamental voltage of Phase A decreased to 1.724 pu for a duration of 0.03 seconds to 0.07 seconds. This is caused by voltage swell. Meanwhile, the fundamental voltage of Phase B decreased to 1.72 pu for a duration of 0.03 to 0.07 seconds. Then, the fundamental voltage of Phase C decreased to 1.694 pu for a duration of 0.03 to 0.07 seconds.

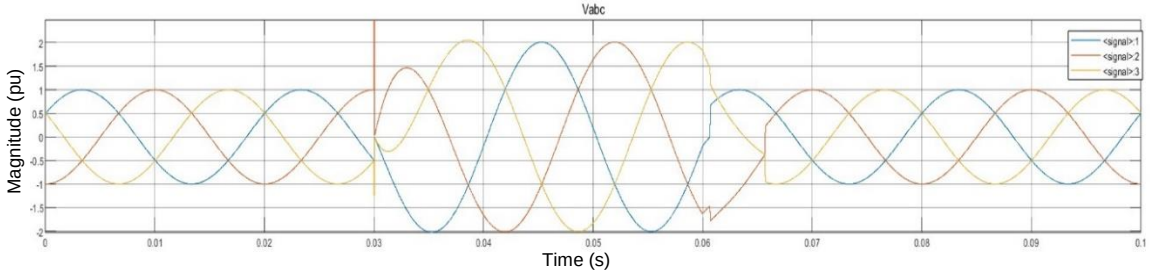

Figure 11. Voltage swell due to 3 phase short circuit

3.5.2. After DVR installation at voltage swell

The simulation was conducted for a 3-phase short circuit fault with a load of 70% and a fault location point of 75%, as shown in Figure 12. The voltage values of phases A, B, and C that experience voltage swell can be determined using the FFT tools in Simulink MATLAB, as shown in Figures 12. The fundamental voltage of Phase A decreased to 0.9989 pu for a duration of 0.03 to 0.07 seconds. This is caused by voltage swell. Meanwhile, the fundamental voltage of Phase B decreased to 0.9965 pu for a duration of 0.03 to 0.07 seconds. Then, the fundamental voltage of Phase C decreased to 1.00 pu for a duration of 0.03 to 0.07 seconds.

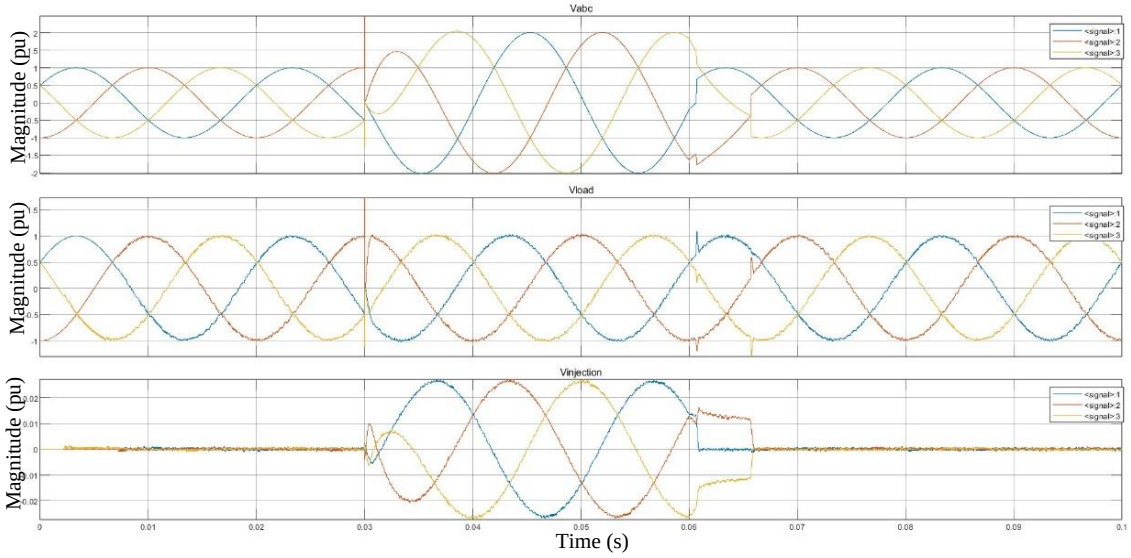

Figure 12. Voltage swell simulation results with DVR

3.5.3. After DSTATCOM installation at voltage swell

The simulation was conducted for a 3-phase short circuit fault with a load of 70% and a fault location point of 75%, as shown in Figure 13. The voltage values of phases A, B, and C that experience voltage swell can be determined using the FFT tools in Simulink MATLAB, as shown in Figures 13. The fundamental voltage of Phase A decreased to 1.269 pu for a duration of 0.03 to 0.07 s. This is caused by voltage swell. Meanwhile, the fundamental voltage of Phase B decreased to 1.26 pu for a duration of 0.03 to 0.07 s. Then, the fundamental voltage of Phase C decreased to 1.253 pu for a duration of 0.03 to 0.07 s.

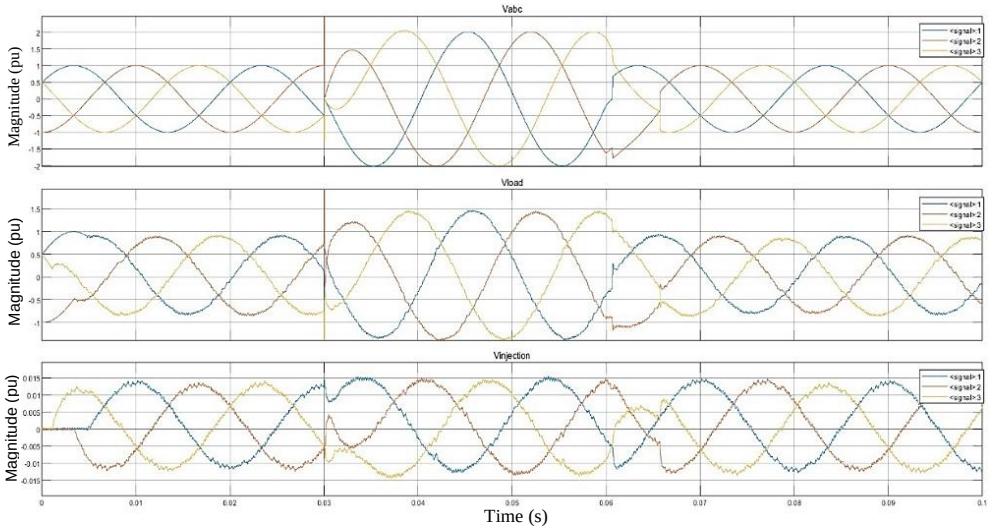

Figure 13. Voltage swell simulation results with DVR

3.5.4. After UPQC-S installation at voltage swell

Simulations were carried out for a 3-phase short circuit fault with a load of 70% and a fault location point of 75% after installing UPQC-S as a lost voltage restorer. The simulation results are shown in Figure 14. The voltage values for phases A, B, and C recovered using UPQC-S can be determined using the FFT tools in Simulink MATLAB, as shown in Figures 14. The fundamental voltage of Phase A is 342.8 V for a duration of 0.03 to 0.07 seconds, so the fundamental voltage of Phase A is 0.9021 pu (reference voltage 380 V). Then, the fundamental voltage of Phase B is 344 V (0.9052 pu) for a time duration of 0.03 to 0.07 seconds. Further, the fundamental voltage of Phase C is 339.7 V (0.8939 pu) for a duration of 0.03 to 0.07 seconds.

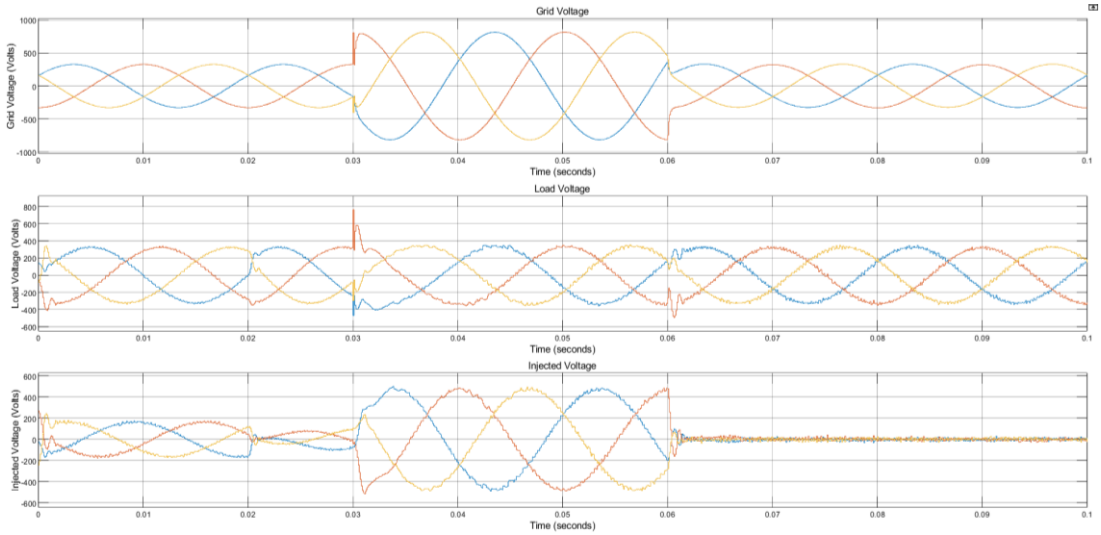

Figure 14. Voltage swell simulation results with UPQC-S

3.6. Summary of analysis of voltage sag simulation results

Based on the results of the voltage sag simulation, which was run at 70% load and 75% fault location point, DVR, DSTATCOM, and UPQC-S can restore the voltage due to voltage sag on the disturbed phase. The simulation results are shown in Table 7. Table 7 presents the simulation results, a crucial step in our research. Before and after the installation of DVR, DSTATCOM, and UPQC-S, we observed a significant voltage sag of 15002 V or 0.75 pu during a 3-phase short circuit. The voltage measured during the sag ranged from 0.25 to 0.30 pu. The selected disturbance duration for the voltage sag simulation was 0.03 to 0.07 seconds, providing a comprehensive view of the response and wave shape during a short circuit fault.

Table 7. Voltage sag compensation simulation results

Phase	V fundamental No compensation	V fundamental DVR	V fundamental DSTATCOM	V fundamental UPQC-S
A	0.3018	0.9679	0.7369	0.8392
B	0.2647	0.966	0.7235	0.8078
C	0.2481	0.9776	0.7167	0.8389

Before compensation, it can see a decrease in system voltage of up to 0.3018 pu in phase A, 0.2647 pu in phase B, and phase C 0.2481 pu. This condition indicates a voltage drop of more than 10% of the nominal voltage in the system and does not meet the standards. After installing the DVR on the system, the voltage was successfully restored to reach 0.9679 pu on phase A, 0.966 pu on phase B, and 0.9776 pu on phase C. After installing DSTATCOM on the system, the voltage was successfully injected until it reached 0.7369 pu on phase A, 0.7235 pu on phase B, and 0.7167 pu on phase C. After installing UPQC-S on the system, the voltage was successfully injected until it reached 0.8392 pu on phase A, 0.8078 pu on phase B, and 0.8389 pu on phase C. Based on the data obtained after carrying out the simulation, it can be seen that the voltage sag disturbance due to a 3-phase short circuit is serious because it causes a decrease of up to 0.25 pu to 0.30 pu. DVR testing injected voltage up to 0.7295 pu to the normal voltage limit of ≥0.9 pu. DSTATCOM testing only injects a voltage of 0.4686 pu to a voltage limit of ≥0.7 pu. Meanwhile, in the UPQC-S test, it succeeded in injecting a voltage of 0.5911 pu to a voltage limit of ≥0.8 pu. These results follow previous research about voltage sag. The addition of DVR, DSTATCOM, and UPQC-S produced better values before compensation [27]–[30].

After conducting tests comparing the installation of a DVR, distribution static compensator, and unified power quality conditioner-series shunt against voltage sag, we found that the DVR is the most suitable solution for the SB-02 Sibolga Feeder case study. The quality of the DVR's voltage injection is superior, successfully restoring the voltage to close to the nominal voltage of 1 pu. In future research, it is possible to increase the efficiency of the harmonic filter on the DVR.

3.7. Summary of analysis of voltage swell simulation results

Based on the results of the voltage sag simulation, which was run at 70% load and 75% fault location point, DVR, DSTATCOM, and UPQC-S can restore the voltage due to voltage swell on the disturbed phase. The simulation results are shown in Table 8. Table 8 shows the simulation results before and after DVR, DSTATCOM, and UPQC-S installation. The calculation results of the voltage swell when a 3-phase short circuit occurs are 15,002 V or 0.75 pu. Based on simulations, the amount of voltage measured during a voltage swell is 1.60 pu to 1.75 pu. In the voltage swell simulation, the selected disturbance duration occurs in the range of 0.03 to 0.07 seconds to see how the response and wave shape occur when a short circuit fault occurs.

Table 8. Voltage swell compensation simulation results

Phase	V fundamental No compensation	V fundamental DVR	V fundamental DSTATCOM	V fundamental UPQC-S
A	1.724	0.9969	1.269	0.9021
B	1.72	0.9965	1.26	0.9052
C	1.694	1	1.253	0.8939

In the simulation without compensation, it can be seen that the system voltage increases up to 1.724 pu in phase A, 1.72 pu in phase B, and in phase C, 1.694 pu. This condition indicates an increase in voltage in the system of more than 160% of the nominal voltage and does not meet the standards. After installing the DVR on the system, the voltage was successfully restored to reach 0.9969 pu on phase A,

0.9965 pu on phase B, and 1.00 pu on phase C, the voltage was successfully restored to reach 0.9969 pu on phase A, 0.9965 pu on phase B, and 1.00 pu on phase C. After installing UPQC-S on the system, the voltage was successfully injected until it reached 0.8392 pu on phase A, 0.8078 pu on phase B, and 0.8389 pu on phase C. Based on the data obtained after carrying out the simulation, it is clear that the DVR test was a resounding success in restoring the voltage to 0.9776 pu, well within the normal voltage limit of ≥0.9 pu. This success reaffirms the DVR's performance. The DSTATCOM testing only reduced the voltage to 1.26 pu on the network, while the UPQC-S test also succeeded in restoring the voltage to 0.9021 pu, meeting the normal voltage limit of ≥0.9 pu. These results follow previous research about voltage swell. The addition of DVR, DSTATCOM, and UPQC-S produced better values before compensation [8], [11], [13]

Based on tests carried out by comparing the installation of DVR, DSTATCOM, and UPQC-S against voltage swell, we can draw insightful conclusions. The results have shown that the DVR is more suitable for use in the SB-02 Sibolga Feeder case study research. This is because the DVR's voltage repair quality is greater, and it succeeds in restoring the voltage to close to the nominal voltage, namely 1 pu. This comparison provides valuable knowledge for future system installations.

4. CONCLUSION

The following conclusions were drawn from the discussion and research conducted: First, the smallest voltage drop, 0.2481 pu on phase C, was caused by the voltage sag that resulted from a three-phase short circuit fault based on a load of 70%, and the fault location point is 75%. Second, the biggest increase in the voltage fundamental wave, reaching 1.724 pu on phase A, was caused by a three-phase short circuit fault with a 70% load and a 75% fault location point. Third, using a 70% load and a 75% fault localization point, the DVR restored the voltage caused by a 3-phase short circuit failure on the SB 02 feeder. The simulation findings show that phase C experiences the largest voltage sag recovery, 0.7295 pu from 0.2481 pu to 0.9776 pu. Additionally, phase A experienced the largest voltage swell recovery, going from 1.724 pu to 0.9969 pu, or 0.7271 pu. Fourth, a three-phase short circuit caused DSTATCOM to restore voltage. The simulation findings show that phase C experiences the largest voltage sag recovery, 0.4686 pu from 0.2481 pu to 0.7167 pu. Additionally, phase B experienced the largest voltage swell recovery, going from 1.7 pu to 1.26 pu, or 0.46 pu. Fifth, a three-phase short circuit allowed UPQC-S to restore voltage successfully. According to the simulation results, phase A experienced the largest voltage sag recovery, rising from 0.2481 pu to 0.8392 pu, or 0.5911 pu. Additionally, phase A had the largest voltage swell recovery, going from 1.724 pu to 0.9021 pu, or 0.8219 pu. Ultimately, it is evident from the research that the DVR is more dependable than the distribution static compensator and unified power quality conditioner-series shunt in mitigating the effects of 3-phase short circuit disturbances on voltage sag and swell.

REFERENCES

[1] S. S. Bhosale, Y. N. Bhosale, U. M. Chavan, and S. A. Malvekar, "Power quality improvement by using UPQC: a review," in *2018 International Conference on Control, Power, Communication and Computing Technologies (ICCPCCT)*, Mar. 2018, pp. 375–380, doi: 10.1109/ICCPCCT.2018.8574264.

[2] R. E. Brown, *Electric Power Distribution Reliability*. CRC Press, 2002, doi: 10.1201/9780824744281.

[3] T. Gonen, *Electric Power Distribution Engineering*. Boca Raton: CRC Press, 2015, doi: 10.1201/b16455.

[4] Amirullah, Adiananda, O. Penangsang, and A. Soeprijanto, "A dual UPQC to mitigate sag/swell, interruption, and harmonics on three phase low voltage distribution system," in *2020 Third International Conference on Vocational Education and Electrical Engineering (ICVEE)*, Oct. 2020, pp. 1–6, doi: 10.1109/ICVEE50212.2020.9243245.

[5] Y. Siregar, Z. Pane, and R. Sipahutar, "Optimization of distributed generating power placement and capacity on the distribution network for voltage stability improvement," in *2021 5th International Conference on Electrical, Telecommunication and Computer Engineering (ELTICOM)*, Sep. 2021, pp. 168–173, doi: 10.1109/ELTICOM53303.2021.9590108.

[6] Y. Siregar, A. A. Azhari Nasution, M. K. Suan Tial, N. Mubarakah, and S. Soeharwinto, "Dynamic voltage restorer performance analysis using fuzzy logic controller and battery energy storage system for voltage sagging," *International Journal of Electrical and Computer Engineering*, vol. 14, no. 2, p. 1215, Apr. 2024, doi: 10.11591/ijece.v14i2.pp1215-1227.

[7] S. K. Yadav, A. Patel, and H. D. Mathur, "Comparison of power losses for different control strategies of UPQC," in *2020 IEEE 9th Power India International Conference (PIICON)*, Feb. 2020, pp. 1–6, doi: 10.1109/PIICON49524.2020.9113005.

[8] R. Pandya and F. Bhavsar, "Study on compensation of voltage sag and voltage swell by using DVR (dynamic voltage restorer)," in *2018 International Conference on Current Trends towards Converging Technologies (ICCTCT)*, Mar. 2018, pp. 1–4, doi: 10.1109/ICCTCT.2018.8550973.

[9] M. F. Shaikh, A. M. Shaikh, S. A. Shaikh, Z. H. Khand, D. Kumar, and R. Nadeem, "Analysis and mitigation of harmonics using C-type high pass filter and improvement of voltage sag with DVR including distributed generation," in *2022 Global Conference on Wireless and Optical Technologies (GCWOT)*, Feb. 2022, pp. 1–9, doi: 10.1109/GCWOT53057.2022.9772922.

[10] Y. Xu, X. Xiao, Y. Sun, and Y. Long, "Voltage sag compensation strategy for unified power quality conditioner with simultaneous reactive power injection," *Journal of Modern Power Systems and Clean Energy*, vol. 4, no. 1, pp. 113–122, Jan. 2016, doi: 10.1007/s40565-016-0183-x.

[11] C. R. Reddy, A. G. Prasad, D. C. Sekhar, B. S. Goud, K. Kumari, and M. D. Kumar, "Voltage sag and swell compensation in integrated system using advanced UPQC," in *2021 International Conference on Decision Aid Sciences and Application (DASA)*, Dec. 2021, pp. 419–423, doi: 10.1109/DASA53625.2021.9682233.

[12] Z. Elkady, N. Abdel-Rahim, A. Mansour, and F. Bendary, "Voltage sag/swell detection based on decoupled stationary reference frame PLL in DVR," in *2021 22nd International Middle East Power Systems Conference (MEPCON)*, Dec. 2021, pp. 678–682, doi: 10.1109/MEPCON50283.2021.9686301.
[13] S. N. Setty, M. S. D. Shashikala, and K. T. Veeramanju, "Hybrid control mechanism-based DVR for mitigation of voltage sag and swell in solar PV-based IEEE 33 bus system," *International Journal of Power Electronics and Drive Systems*, vol. 14, no. 1, pp. 209-221, Mar. 2023, doi: 10.11591/ijpeds.v14.i1.pp209-221.
[14] P. N. Jaiswal, K. Thakre, and P. Nigam, "Comparison of DSTATCOM, DVR and UPQC for mitigating voltage sag in distribution system," in *2022 IEEE 2nd International Symposium on Sustainable Energy, Signal Processing and Cyber Security (iSSSC)*, Dec. 2022, pp. 1–6, doi: 10.1109/iSSSC56467.2022.10051621.
[15] H. Ghosh, P. Kumar Saha, and G. Kumar Panda, "Performance comparison between DVR and DSTATCOM used for load voltage control in distribution side," in *2012 International Conference on Advances in Power Conversion and Energy Technologies (APCET)*, Aug. 2012, pp. 1–6, doi: 10.1109/APCET.2012.6302026.
[16] S. Singh, V. Rai, A. Kumar, and K. B. Sahay, "Simulation and comparison of DVR and D-STATCOM for voltage sag mitigation," in *2016 IEEE 6th International Conference on Power Systems (ICPS)*, Mar. 2016, pp. 1–6, doi: 10.1109/ICPES.2016.7584238.
[17] Y. Siregar, M. Muhammad, Y. Z. Arief, N. Mubarakah, S. Soeharwinto, and R. Dinzi, "Dynamic voltage restorer quality improvement analysis using particle swarm optimization and artificial neural networks for voltage sag mitigation," *International Journal of Electrical and Computer Engineering*, vol. 13, no. 6, p. 6079, Dec. 2023, doi: 10.11591/ijece.v13i6.pp6079-6091.
[18] N. Abas, S. Dilshad, A. Khalid, M. S. Saleem, and N. Khan, "Power quality improvement using dynamic voltage restorer," *IEEE Access*, vol. 8, pp. 164325–164339, 2020, doi: 10.1109/ACCESS.2020.3022477.
[19] B. L. S. Shraddha, S. R, S. J. Pillai, and S. Modi, "Simulation and analysis of dynamic voltage restorer," in *2018 3rd IEEE International Conference on Recent Trends in Electronics, Information & Communication Technology (RTEICT)*, May 2018, pp. 1388–1393, doi: 10.1109/RTEICT42901.2018.9012532.
[20] B. Srilakshmi, K. Sudharshan Reddy, H. C. Mahadeva, and M. Gayathri, "Power quality improvement using dynamic voltage restorer," in *2018 3rd IEEE International Conference on Recent Trends in Electronics, Information & Communication Technology (RTEICT)*, May 2018, pp. 558–561, doi: 10.1109/RTEICT42901.2018.9012583.
[21] T. Karthik, M. Prathyusha, R. Thirumalaivasan, and M. Janaki, "Power quality improvement using DSTATCOM," in *2019 Innovations in Power and Advanced Computing Technologies (i-PACT)*, Mar. 2019, pp. 1–7, doi: 10.1109/i-PACT44901.2019.8960234.
[22] V. K. Govil, K. Sahay, and S. M. Tripathi, "A Survey on DSTATCOM control and power quality improvement techniques," in *2022 1st International Conference on Sustainable Technology for Power and Energy Systems (STPES)*, Jul. 2022, pp. 1–6, doi: 10.1109/STPES54845.2022.10006454.
[23] M. A. Kallon, G. N. Nyakoe, and C. M. Muriithi, "DSTATCOM application for distribution network power quality enhancement: a review," in *2021 IEEE PES/IAS PowerAfrica*, Aug. 2021, pp. 1–5, doi: 10.1109/PowerAfrica52236.2021.9543214.
[24] V. Gundeboina, R. R. Chilipi, and S. Arya, "Power quality enhancement using UPQC-S with multiple adaptive noise cancellation filters," in *2022 IEEE 2nd International Conference on Sustainable Energy and Future Electric Transportation (SeFeT)*, Aug. 2022, pp. 1–5, doi: 10.1109/SeFeT55524.2022.9909174.
[25] A. Sharma, S. K. Sharma, and B. Singh, "Unified power quality conditioner analysis design and control," in *2018 IEEE Industry Applications Society Annual Meeting (IAS)*, Sep. 2018, pp. 1–8, doi: 10.1109/IAS.2018.8544566.
[26] D. M. Matlani and M. D. Solanki, "UPQC: an exhaustive solution to improve power quality," in *2020 4th International Conference on Electronics, Communication and Aerospace Technology (ICECA)*, Nov. 2020, pp. 416–421, doi: 10.1109/ICECA49313.2020.9297522.
[27] A. H. Soomro, A. S. Larik, M. A. Mahar, A. A. Sahito, and I. A. Sohu, "Simulation-based analysis of a dynamic voltage restorer under different voltage sags with the utilization of a PI controller," *Engineering, Technology & Applied Science Research*, vol. 10, no. 4, pp. 5889–5895, Aug. 2020, doi: 10.48084/etasr.3524.
[28] M. A. El-Gammal, A. Y. Abou-Ghazala, and T. I. El-Shennawy, "Dynamic voltage restorer (DVR) for voltage sag mitigation," *International Journal on Electrical Engineering and Informatics*, vol. 3, no. 1, pp. 1–11, Mar. 2011, doi: 10.15676/ijeei.2011.3.1.1.
[29] S. S. Kishore, S. K. Sinha, P. Abirami, and M. L. George, "Voltage sag reduction and power quality improvement using DVR," in *2017 International Conference on Computation of Power, Energy Information and Communication (ICCPEIC)*, Mar. 2017, pp. 761–767, doi: 10.1109/ICCPEIC.2017.8290465.
[30] A. M. Rauf and V. Khadkikar, "An enhanced voltage sag compensation scheme for dynamic voltage restorer," *IEEE Transactions on Industrial Electronics*, vol. 62, no. 5, pp. 2683–2692, May 2015, doi: 10.1109/TIE.2014.2362096.

BIOGRAPHIES OF AUTHORS

Yulianta Siregar was born July 09, 1978 in Medan, North Sumatera Utara, Indonesia. He did his undergraduate work at University of Sumatera Utara in Medan, North Sumatera Utara, Indonesia. He received a bachelor of engineering in 2004. After a while, he worked for a private company. He continued taking a master's program in electrical engineering at the Institute of Sepuluh Nopember, Surabaya, West Java, Indonesia, from 2007-2009. He was in a Ph.D. program at Kanazawa University, Japan, from 2016-2019. Until now, he lectured at Universitas Sumatera Utara. He can be contacted at email: julianta_srg@usu.ac.id.

Syahrun Mubarok is a fresh graduate of electrical engineering bachelor's degree from Universitas Sumatera Utara in 2024. His research area field study is an electrical power system. He can be contacted at email: syahrunmubarok99@gmail.com.

Nur Nabila Mohamed was born in Pontianak, Indonesia, in 1971. She graduated from Department on Electronic Information System, College of Systems Engineering, Shibaura Institute of Technology, Oomiya Campus, Japan, in 2012. He received the M.Sc. degree from Universiti Teknologi MARA (UiTM), Malaysia, with thesis title is "Symmetric encryption using pre-shared public parameters for a secure trivial file transfer protocol," and the Ph.D. degree from Universiti Teknologi MARA (UiTM), Malaysia, with thesis title is "Packet header support using hybrid security approach for securing trivial file transfer protocol (TFTP) in machine-to-machine application." His research interests include network security, information security, internet of things. Currently he is a senior lecturer of electrical engineering, college of engineering, University Technology MARA, Shah Alam Selangor. He can be contacted at email address: nurnabilamohamed@uitm.edu.my.